Development 140, 136-146 (2013) doi:10.1242/dev.087791

Genetic elevation of Sphingosine 1-phosphate suppresses dystrophic muscle phenotypes in *Drosophila*

Mario Pantoja[1], Karin A. Fischer[1], Nicholas Ieronimakis[2], Morayma Reyes[2,3] and Hannele Ruohola-Baker[1,*]

SUMMARY

Duchenne muscular dystrophy is a lethal genetic disease characterized by the loss of muscle integrity and function over time. Using *Drosophila*, we show that dystrophic muscle phenotypes can be significantly suppressed by a reduction of *wunen*, a homolog of lipid phosphate phosphatase 3, which in higher animals can dephosphorylate a range of phospholipids. Our suppression analyses include assessing the localization of Projectin protein, a titin homolog, in sarcomeres as well as muscle morphology and functional movement assays. We hypothesize that *wunen*-based suppression is through the elevation of the bioactive lipid Sphingosine 1-phosphate (S1P), which promotes cell proliferation and differentiation in many tissues, including muscle. We confirm the role of S1P in suppression by genetically altering S1P levels via reduction of S1P lyase (*Sply*) and by upregulating the serine palmitoyl-CoA transferase catalytic subunit gene *lace*, the first gene in the *de novo* sphingolipid biosynthetic pathway and find that these manipulations also reduce muscle degeneration. Furthermore, we show that reduction of *spinster* (which encodes a major facilitator family transporter, homologs of which in higher animals have been shown to transport S1P) can also suppress dystrophic muscle degeneration. Finally, administration to adult flies of pharmacological agents reported to elevate S1P signaling significantly suppresses dystrophic muscle phenotypes. Our data suggest that localized intracellular S1P elevation promotes the suppression of muscle wasting in flies.

KEY WORDS: Muscular dystrophy, Sphingosine 1-phosphate, LPP3

INTRODUCTION

Duchenne muscular dystrophy (DMD) is an age-dependent muscle wasting disease caused by the absence of fully functional dystrophin protein. This severe X-linked recessive disease affects 1 in 3500 male births (Deconinck and Dan, 2007). In human dystrophic muscles, rounds of contractions result in degeneration/regeneration cycles. However, regeneration is not sufficient to overcome degeneration in dystrophic muscles, leading to muscle wasting over time. As no effective treatment exists presently, new approaches are imperative (Mendell et al., 2010; Palmieri et al., 2010). Genetically amenable models for DMD might allow identification of new components that interact with the dystrophin glycoprotein complex.

Presently, several mammalian animal models, including mouse, dog and cat, have been established to study the disease (Collins and Morgan, 2003). More recently, genetically tractable DMD models have also been established in zebrafish, *Caenorhabditis elegans* and *Drosophila melanogaster* (Collins and Morgan, 2003; Shcherbata et al., 2007). Among the dystrophic phenotypes observed in *Drosophila* is a visible wing vein defect (Christoforou et al., 2008; Kucherenko et al., 2008), which was previously used to screen for suppressors (Kucherenko et al., 2008). One of the suppressors of the wing vein defect was mutant of *wunen*, a lipid phosphate phosphatase, which was initially identified as a gene required for proper germ cell migration in the *Drosophila* embryo (Zhang et al., 1996; Zhang et al., 1997; Starz-Gaiano et al., 2001). There are three lipid phosphate phosphatases in mammals: LPP1, LPP2 and LPP3 (also known as PPAP2A, PPAP2C and PPAP2B, respectively). Rescue analysis revealed that human LPP3 acts as a functional homolog of *wunen* in germ cell migration (Burnett and Howard, 2003). It is noteworthy that despite having the same broad substrate range *in vitro*, acting upon phosphatidic acid (PA), sphingosine 1-phosphate (S1P) and their derivatives (Pyne et al., 2005), only *Lpp3* knockout mice are embryonic lethal indicating a necessary central role for this enzyme in development (Brindley and Pilquil, 2009). Interestingly, it has been reported that LPP2 preferentially attenuates intracellular PA levels whereas LPP3 specifically attenuates intracellular levels of S1P in human cells (Long et al., 2005), indicating a preference for this substrate.

Human LPP3 is a secreted protein and has its active site either in the extracellular space or in the lumen of intracellular organelles, yet it affects intracellular levels of S1P. This presumably occurs through inter-compartmental movement of S1P via a transporter such as *SPNS2*, a member of the major facilitator family of transporters that has been shown to specifically transport S1P (Osborne et al., 2008; Kawahara et al., 2009; Hisano et al., 2011).

S1P has been implicated in muscle repair and satellite cell proliferation and myoblast differentiation *in vitro* (Nagata et al., 2006; Bruni and Donati, 2008; Rapizzi et al., 2008). Here, we show that, in *Drosophila*, *wunen* reduction, in addition to suppressing the wing vein defect, also suppresses dystrophic muscle defects as assayed by muscle integrity, Projectin (Bent – FlyBase) protein localization in sarcomeres, and fly movement over time. Furthermore, mutants that increase intracellular S1P levels either biochemically or through the reduction of transport also suppress these dystrophic muscle phenotypes in *Drosophila*. Finally, elevating S1P or S1P signaling in adult flies using pharmacological agents phenocopied the genetic data.

[1]Department of Biochemistry, Institute for Stem Cell and Regenerative Medicine, University of Washington, Seattle, WA 98195, USA. [2]Department of Pathology, School of Medicine, University of Washington, Seattle, WA 98195, USA. [3]Department of Laboratory Medicine, School of Medicine, University of Washington, Seattle, WA 98195, USA.

*Author for correspondence (hannele@u.washington.edu)

Accepted 8 October 2012

MATERIALS AND METHODS

Fly stocks

The fly strains used in this study are: *Oregon-R*, w^{1118}, Dys^{det1}, wun^{EMS4}/*CyO*, *yw*, *TubGal4/TM3*, cn^1Sply^{05091}/*CyO;* ry^{506}, *Df(3R)Exel6184/TM6B* (outcrossed to w^{1118} at least seven times in this laboratory) and $wun^{EY11935}$, all obtained from the Bloomington Stock Center; *w*; *UAS-HA-lace/CyO* kindly provided by Dr T. Adachi-Yamada (Gakushuin University, Tokyo, Japan); *w*; wun^{k10201}/CyO (stock #111469) obtained from the Kyoto *Drosophila* Genetic Resource Center; wun^{RNAi} [w^{1118}; *P{GD1640}v6446/TM3* (stock #6446)] obtained from the Vienna *Drosophila* RNAi Center (Dietzl et al., 2007); *ActGal4:UAS-*$Dys^{N\text{-}RNAi}$*/CyO* and *TubGal4:UAS-*$Dys^{C\text{-}RNAi}$*/TM6B, Tb* recombinant lines, previously generated in this laboratory (Kucherenko et al., 2008); and SK1 and SK2 RNAi lines obtained from the Vienna *Drosophila* RNAi Center (stock numbers v32932 and v101018, respectively).

Myofibril immunohistochemistry

Flies were dipped in 95% ethanol and then dissected in 1× PBS (pH 7.4). Heads and abdomens were removed, and the thoraces opened. Samples were then fixed in 5% paraformaldehyde (Electron Microscopy Sciences) at room temperature (RT) for 1 hour with rocking, rinsed in PBT [PBS with 0.2% Triton X-100 (v/v)] four times (15 minutes each), and then blocked for 1 hour in PBTB [PBT with 0.4% bovine serum albumin (w/v), 5% normal goat serum (v/v)] at RT. Samples were stained with primary antibody pre-diluted in PBTB [rat anti-Projectin (Mac150), Babraham Institute; 1:50] overnight at 4°C with rocking, rinsed in PBT four times (10 minutes each) at RT, and then stained with secondary antibody pre-diluted in PBTB (Alexa Fluor 488-conjugated goat anti-rat at 1:500 and Alexa-Fluor 568-conjugated goat anti-mouse anti-Phalloidin at 1:200; Invitrogen) overnight at 4°C with rocking. Samples were then rinsed in PBT four times (10 minutes each) at RT and stored in 80% glycerol (v/v), 3% n-propyl gallate (w/v), 20% Prolong Gold (Invitrogen) (v/v). Individual indirect flight muscles (IFMs) were mounted on slides using forceps to spread them evenly and then coverslipped. Analysis was carried out using a Leica TCS-SPE confocal microscope with a 40× objective and Leica Software. Myofibrils were quantified as percentage wild type (WT) out of total number analyzed. For each myofibril, a confocal projection was scored WT or non-WT where WT was recorded when Projectin staining continuously spanned the entire width of the myofibril. For each genotype, four to five flies were analyzed, and six to seven myofibrils from three different IFMs (approximately two myofibrils per IFM) per fly were analyzed.

Indirect flight muscle histology

Transverse histological sections of IFMs were prepared from paraffin wax-embedded material. Flies were immobilized in Heisenberg fly collars (Model #10731, 4M Instrument & Tool LLC, New York) between the abdomen and thorax, then fixed in Carnoy's solution [6:3:1 ethanol (EtOH):chloroform:glacial acetic acid] overnight at 4°C. After fixation, at RT, samples were hydrated/dehydrated to remove the Carnoy's with the following procedure: 40% EtOH (10 minutes), 75% EtOH (10 minutes), 95% EtOH (10 minutes), then 100% EtOH twice (10 minutes each). The flies were then infiltrated with paraffin (Poly/Fin, Triangle Biomedical Sciences) using the following procedure: samples were placed in methyl benzoate for 30 minutes at 65°C, then transferred to a methyl benzoate:paraffin solution (1:1) and incubated at 65°C for 30 minutes, and finally placed in paraffin alone at 65°C for an additional 30 minutes. Afterwards, samples were placed in casts then filled with melted paraffin (65°C). Once cooled and solidified, the collars were removed, shearing off the fly abdomens. Transverse sections of the fly thoraces were cut with a rotary microtome (Leica 820 Histocut) at 10 µm thickness. Paraffin was removed with xylene (two 4-minute immersions) and the sections were rehydrated [100% EtOH twice (4 minutes each), 95% EtOH (3 minutes), 70% EtOH (2 minutes), H_2O (1 minute)] then stained with Hematoxylin and Eosin using standard protocols. Sections were covered with DPX Mountant (Fluka), coverslipped and analyzed by light microscopy (Leica) using the 20× objective. The middle third (15-20 sections) of the thorax, cut in 10 µm sections, of each fly was scored for degeneration. Each section was rated A-E depending on the severity of the fragmentation phenotype as follows: (A) more than two of the IFMs were unfragmented; (B) at least one IFM was unfragmented; (C) fragmentation in all IFMs; (D) severe degeneration in at least one IFM; (E) severe degeneration in more than one IFM. A muscle integrity index (MII) was then calculated. The MII is a weighted average of sections showing less degeneration over time (A=16, B=8, C=4, D=2 and E=0). Each fly was given an overall score from ~20 sections. Eight to twelve flies were scored for each experiment; each experiment was repeated three times.

Climbing assay

An apparatus made for fractionating a *Drosophila* population using a countercurrent distribution procedure (Benzer, 1967) was used to measure climbing ability of different fly cohorts. The apparatus was a kind loan from Leo Pallanck (University of Washington, WA, USA). Twenty to thirty flies were tested for their ability to climb at least 10 cm in 30 seconds. Each group of flies was tested for five trials with 3 minutes separating each trial and this denoted a single experiment. Each set of five trials was then given a climbing index (CI) value. The CI is a weighted average of the number of flies that end up in progressively more distant tubes from the first tube of the apparatus. Weighted values were 0, 2, 4, 8, 16, 32 from the first to the last tube, respectively. Each experiment was repeated three times.

Activity assay

A TriKinetics DAM5 activity monitoring system was used to record the movements of individual flies over the course of different lengths of time. The monitors were placed at 38° angles with the food at the bottom of the glass tubes. Seven to eight flies were monitored for each genotype per experiment. Data for the one or two least active flies for each genotype was removed leaving data for the six most active flies per experiment. Each experiment was repeated three times.

Feeding assay

For the feeding assay, 4-day-old (or 0-day-old for long term experiments) flies were placed in empty vials and starved for 6 hours. The flies were then provided access to a solution of 0.05 mg/ml (217 µM) 2-acetyl-4(5)-tetrahydroxybutyl imidazole (THI) in 5% light corn syrup (Karo) in either PBS (pH 7.4) or water for 16-18 hours. The flies were placed in new, yeasted vials for 6-7 hours. Flies were then transferred to empty vials with access to a solution of 0.05 mg/ml THI in a 5% light corn syrup solution, as before, for 16-18 hours. This was repeated for a third time (or for 14 days for long term experiments). The flies were then placed in new, yeasted vials and if not analyzed immediately were transferred to new, yeasted vials daily before myofibril or activity analysis. The protocol described above was followed for THI oxime: (E)-1-(4-((1R,2S,3R)-1,2,3,4-tetrahydroxybutyl)-1H-imidazol-2-yl)ethanone oxime (LX2931, Lexicon Pharmaceuticals; a gift from Dr Buchynskyy and Prof. Gelb, University of Washington, WA, USA) as well as Fingolimod (FTY720) (Cayman). In these studies, both THI oxime and FTY720 were delivered at the same molar concentration as used for THI, 217 µM.

Statistics

Two-tailed Student's *t*-test was used to determine statistical significance for all experiments.

RESULTS

Establishment of a dystrophic myofibril phenotype

Drosophila Dystrophin (*Dys*) mutants show a variety of dystrophic phenotypes, including muscle, neuronal and heart defects (Shcherbata et al., 2007; Christoforou et al., 2008; Taghli-Lamallem et al., 2008). Here, we extend the muscle analysis to the level of the sarcomere (Perkins et al., 2010; Schnorrer et al., 2010). Two titin-like proteins, Projectin and Kettin (Sallimus – FlyBase), form the connecting filaments in indirect flight muscles (IFMs) that link the Z-bands to thick filaments and function in muscle elasticity during oscillatory work in flight (Lakey et al., 1990; Moore et al., 1999; Ayme-Southgate et al., 2005; Bullard et al., 2006). Because

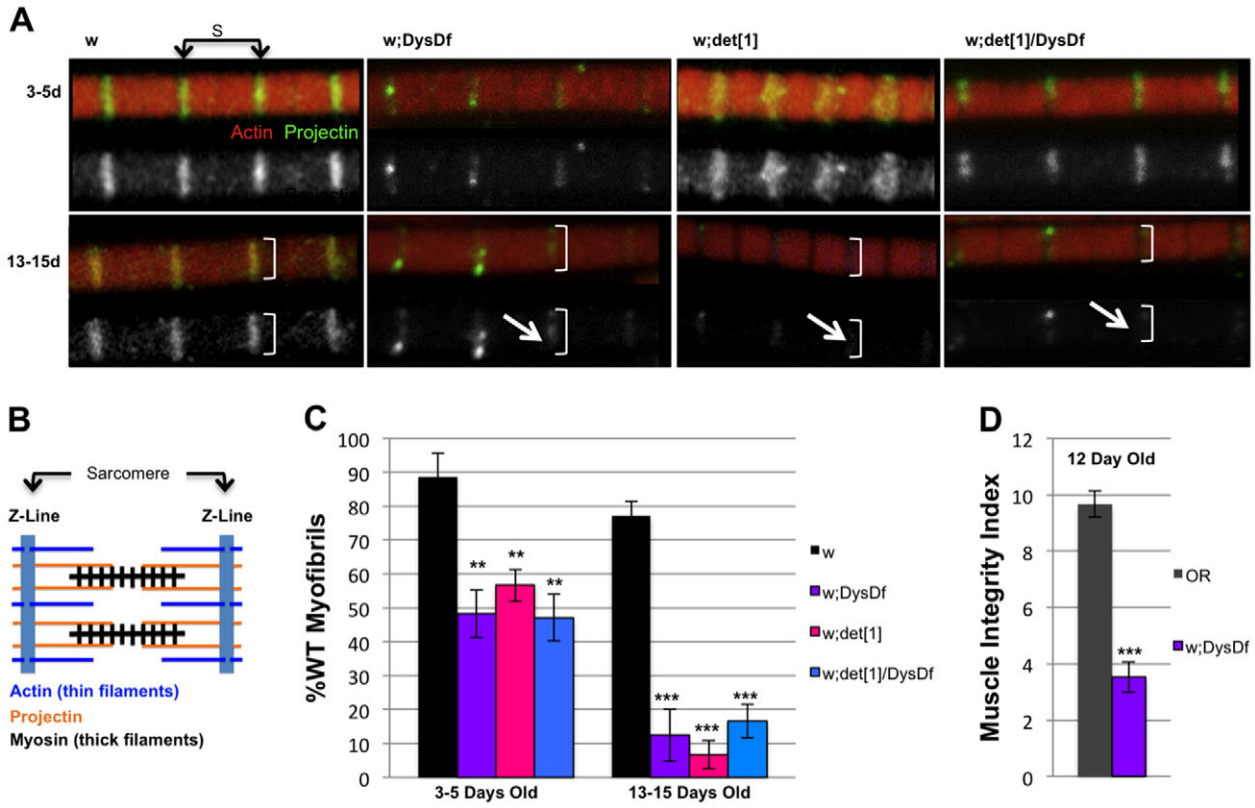

Fig. 1. Age-dependent dystrophic myofibril phenotypes. (**A**) Confocal images of individual IFM myofibrils of 3- to 5-day-old and 13- to 15-day-old flies of wild type (*w*), *w;DysDf*, *w;Dys*^{det1} and *w;DysDf/Dys*^{det1}. Actin (red) and Projectin (green, grayscale). White brackets indicate width of the myofibril. Arrows indicate a representative defective Projectin pattern. S marks the length of one sarcomere. (**B**) Schematic representation of a sarcomere. (**C**) Percentage of wild-type IFM myofibrils from each genotype shown in A at 3-5 days and 13-15 days. (**D**) Quantification of histological section data. Muscle integrity index is a weighted average of scored sections measuring the intactness of the IFMs (see Materials and methods). Ten flies were scored for each experiment; each experiment was repeated three times. ***P*<0.01, ****P*<0.001. Error bars represent s.e.m.

significant degradation of titin has been reported in muscle biopsies of DMD patients (Matsumura et al., 1989) and titin mutations cause muscular dystrophies and cardiomyopathies (Hackman et al., 2002; Udd et al., 2005), we analyzed the expression pattern of a titin-like protein, Projectin, in *Dys* mutant myofibrils. The data reveal that the Projectin pattern is the most sensitive marker for contraction-induced damage in *Drosophila*. Projectin is a large linker protein connecting thick filament myosin to thin filament actin, but the antibody used in these studies specifically recognizes an epitope close to the Z-line producing a sharp banding pattern spanning the entire width of the sarcomere on either side of the Z-line (Fig. 1A,B). Whereas the Projectin expression pattern is defective, other sarcomeric proteins, e.g. actin, tropomyosin and troponin C show normal expression patterns in dystrophic flies over the temporal length (5-15 days) of our analyses (Fig. 1; data not shown).

We used the sarcomere expression pattern of Projectin (Lakey et al., 1990; Ayme-Southgate et al., 2005) to assess myofibril integrity in *DysDf* (a deficiency that removes most of the *Dys* gene), *Dys*^{det1} (a hypomorphic allele) and *Dys*$^{C\text{-}RNAi}$ (*TubGal4:UAS-Dys*$^{C\text{-}RNAi}$/+) animals along with controls at two different time points. Projectin staining in normal myofibrils results in a uniform and intense band that spans the entire myofibril (Fig. 1A, first upper panel). This normal Projectin pattern was already somewhat disrupted in young *Dys* mutant myofibrils (Fig. 1A, second-fourth upper panels). However, the phenotype became significantly more penetrant and stronger in older animals (Fig. 1A, second-fourth lower panels). Phenotypes in young animals ranged from a diffuse Projectin staining on either side of the Z-line to a band that only partly stains the myofibril, whereas phenotypes in older (13- to 15-day-old) *Dys* mutant muscles ranged from highly reduced to punctate, or absent Projectin staining (Fig. 1A, second-fourth lower panels). In quantifying this phenotype at early and late time points (Fig. 1C), wild type is scored when Projectin continuously spans the entire width of the myofibril. However, qualitatively, it appears that we have defined an allelic series of *Dystrophin* mutants (*DysDf/DysDf*>*DysDf/Dys*^{det1}>*Dys*^{det1}/*Dys*^{det1}>*Dys*$^{C\text{-}RNAi}$/+) in which the deficiency is strongest, showing the greatest reduction of Projectin staining, and the RNAi mutant is weakest (Fig. 1A and Fig. 2A, middle panel). The dramatic defect in the pattern of a structural protein of the muscle contraction machinery in *Dys* mutants is consistent with contraction-induced damage over time and shows that the Dystrophin protein is an essential component in maintaining the stability of the molecular architecture of myofibrils. Collectively, these defective myofibrils eventually degrade and lead to a significant increase in fragmentation and degeneration in dystrophic compared with control transverse histological sections of IFMs (Fig. 1D; supplementary material Fig. S1A-E).

Suppression of dystrophic muscle phenotypes by genetically reducing *wunen*

Previously, we have characterized *wunen* as a suppressor of the dystrophic wing vein phenotype (Kucherenko et al., 2008). Here,

we tested whether reduced Wunen could suppress the muscle defects observed in *Dys* mutant animals. Unlike mammals, in which dystrophin is on the X chromosome, the gene is autosomic in flies so it is necessary to make the flies homozygous for *Dys* in addition to reducing the copy number of any gene of interest. However, as we had previously constructed single chromosome *Dystrophin* RNAi mutants (among which was *TubGal4:UAS-Dys$^{C\text{-}RNAi}$*) for screening, we used these animals to more rapidly assess the capacity of *wunen* mutations to suppress dystrophic muscle phenotypes. A significant suppression of the defective, punctate Projectin staining in *Dys$^{C\text{-}RNAi}$* (*TubGal4:UAS-Dys$^{C\text{-}RNAi}$/+*) myofibrils was observed when *wunen* was reduced (Fig. 2A; *UAS-wun^{RNAi}/TubGal4:UAS-Dys$^{C\text{-}RNAi}$*). We observed a fourfold increase in the number of wild-type myofibrils in *Dys$^{C\text{-}RNAi}$* flies, reaching 80% of control levels (Fig. 2C). Moreover, to determine whether this suppression was also observed with classical, DNA-lesion mutant alleles, we tested the capacity of *wun^{k10201}*, a P-element insertion allele, and *wun^{4}*, an ethyl methanesulfonate (EMS)-induced allele, to suppress the myofibril phenotype seen in *DysDf* animals. We found that both *wunen* alleles suppressed the strong loss of Projectin phenotype associated with 5-day-old *DysDf* animals (*wun/CyO*; *DysDf/DysDf*; Fig. 2B,D). These data correlated with the *wunen*-based suppression of the gross morphological muscle defects seen in dystrophic transverse histological sections of IFMs (Fig. 2E-G) and shows that *wunen* reduction suppresses muscle defects in *Dys* mutants.

Suppression of dystrophic muscle phenotypes by genetically increasing S1P levels

To determine whether *wunen*-dependent suppression of the dystrophic muscle phenotypes correlates with the result obtained with elevating S1P, we altered other known components of sphingolipid metabolism using available fly lines to see whether these changes could phenocopy *wunen* suppression. We tested two mutant backgrounds, which should increase S1P levels, for their ability to suppress dystrophic muscle phenotypes. It has been reported in mice that genetic reduction of S1P lyase, which irreversibly removes S1P from sphingosine metabolism by cleaving the compound to hexadecenaldehyde and phosphorylethanolamine, leads to a significant increase in S1P levels (Bagdanoff et al., 2009). Hence, we first constructed dystrophic animals heterozygous for *Sply*, the *Drosophila* S1P lyase gene (Fig. 3A). Interestingly, we found that, like *wunen*, reduction of *Sply* significantly suppressed the loss of Projectin in dystrophic myofibrils (Fig. 3B,C; *Sply/+; TubGal4:UAS-Dys$^{C\text{-}RNAi}$/+*). Also, like *wunen*, reduction of *Sply* suppressed the strong *DysDf* phenotype in 5-day-old animals (Fig. 3D,E). Additionally, like *wunen*, *Sply* reduction suppressed the muscle fragmentation phenotype observed in transverse histological sections of IFMs (Fig. 3G,I).

We next used the *UAS-lace* transgenic fly line (Adachi-Yamada et al., 1999) to test for suppression of muscle degeneration. We reasoned that, when combined with tubulin-Gal4, the *UAS-lace* transgene could theoretically increase S1P levels by upregulating the expression of *lace*, the gene encoding the catalytic subunit of the first protein in the *de novo* synthesis pathway, serine palmitoyl CoA transferase (Fig. 3A). We placed the *UAS-lace*-containing chromosome into the tubulin-Gal4-driven *Dys$^{C\text{-}RNAi}$* background and found that the Projectin expression pattern in myofibrils at 15 days showed a significant suppression of the dystrophic phenotype (Fig. 3B,C; *UAS-lace/+;TubGal4:UAS-Dys$^{C\text{-}RNAi}$/+*). In fact, quantitatively this was the highest level of suppression observed for which the percentage of wild-type myofibrils scored was not significantly different from non-dystrophic control flies (Fig. 3C; *TubGal4/+*). No suppression was observed in the control dystrophic animals (Fig. 3C; *+/CyO; TubGal4:UAS-DysC-RNAi/+*). Similar to reduced *Sply*, the fragmentation defect observed in histological sections of dystrophic flies was significantly suppressed when *lace* was overexpressed (Fig. 3H,I).

We used tubulin-driven RNAi mutants of Sphingosine Kinases 1 and 2 (SK1 and SK2, respectively) to assess whether reduction of S1P could exacerbate the muscle phenotypes in dystrophic flies. Reduction of kinase activity in wild-type backgrounds resulted in viability for SK1 and lethality for SK2. Interestingly, reduction of either kinase in dystrophic flies was lethal (Fig. 3J).

Suppression of the dystrophic myofibril phenotype by genetically reducing *spinster*, a putative S1P transporter

S1P signaling in mammals is much more complex than that observed in *Drosophila*. In mammals, S1P is both an extracellular and intracellular signaling molecule and has been shown to bind five different G protein-coupled receptors (Rosen et al., 2009). There do not appear to be S1P G protein-coupled receptors in flies, so it is reasonable to assume that S1P acts intracellularly as it does in the budding yeast *Saccharomyces cerevisiae* (Strub et al., 2010). Though *Drosophila* do not appear to have S1P receptors, they do have a putative S1P transporter, *spinster*. In fact, the vertebrate homolog that is named for *spinster*, *spinster 2* (*spns2*) has been shown to specifically transport S1P in zebrafish and in human cells (Kawahara et al., 2009; Hisano et al., 2011). This was intriguing to us and we hypothesized that *spinster* could regulate S1P levels by transporting S1P between cellular compartments. Because S1P is generated intracellularly (Breslow and Weissman, 2010) and S1P lyase had been shown to function on the cytoplasmic side of the endoplasmic reticulum (Ikeda et al., 2004), we investigated whether reduction of *spinster* could elevate S1P levels in the cytoplasmic compartment and therefore phenocopy reduction of *Sply* in suppressing the dystrophic myofibril phenotype. We crossed the strong, genetic null *spin^{11F5}* allele into the *TubGal4:UAS-Dys$^{C\text{-}RNAi}$* dystrophic background and assessed the Projectin content of myofibrils of flies at both 5 and 15 days of age (Fig. 4A,B). We found that reduction of *spinster* significantly suppressed the dystrophic myofibril phenotype at the 15-day time point (quantified in Fig. 4B).

Suppression of dystrophic muscle function phenotypes as assessed by fly movement assays

Up to this point we have analyzed the structural and morphological phenotypes associated with muscle degeneration in dystrophic flies. To address S1P-based suppression of the dystrophic muscle function phenotypes seen in dystrophic animals, we utilized fly movement assays: climbing via a countercurrent apparatus (Greene et al., 2003; Shcherbata et al., 2007) and automated monitoring of overall activity (Fig. 5A).

Functionally, dystrophic flies have a reduced climbing ability compared with control flies (Shcherbata et al., 2007; supplementary material Fig. S1G). In this assay, the flies are challenged by being gently tapped to the bottom of a sequential series of tubes and their negative geotactic behavior is used to assess muscle function by measuring how far they climb in 30-second intervals (see Materials and methods). In addition to this assay, we used an experimenter-independent assay to test muscle function by recording the overall activity of animals over time using an automated monitoring

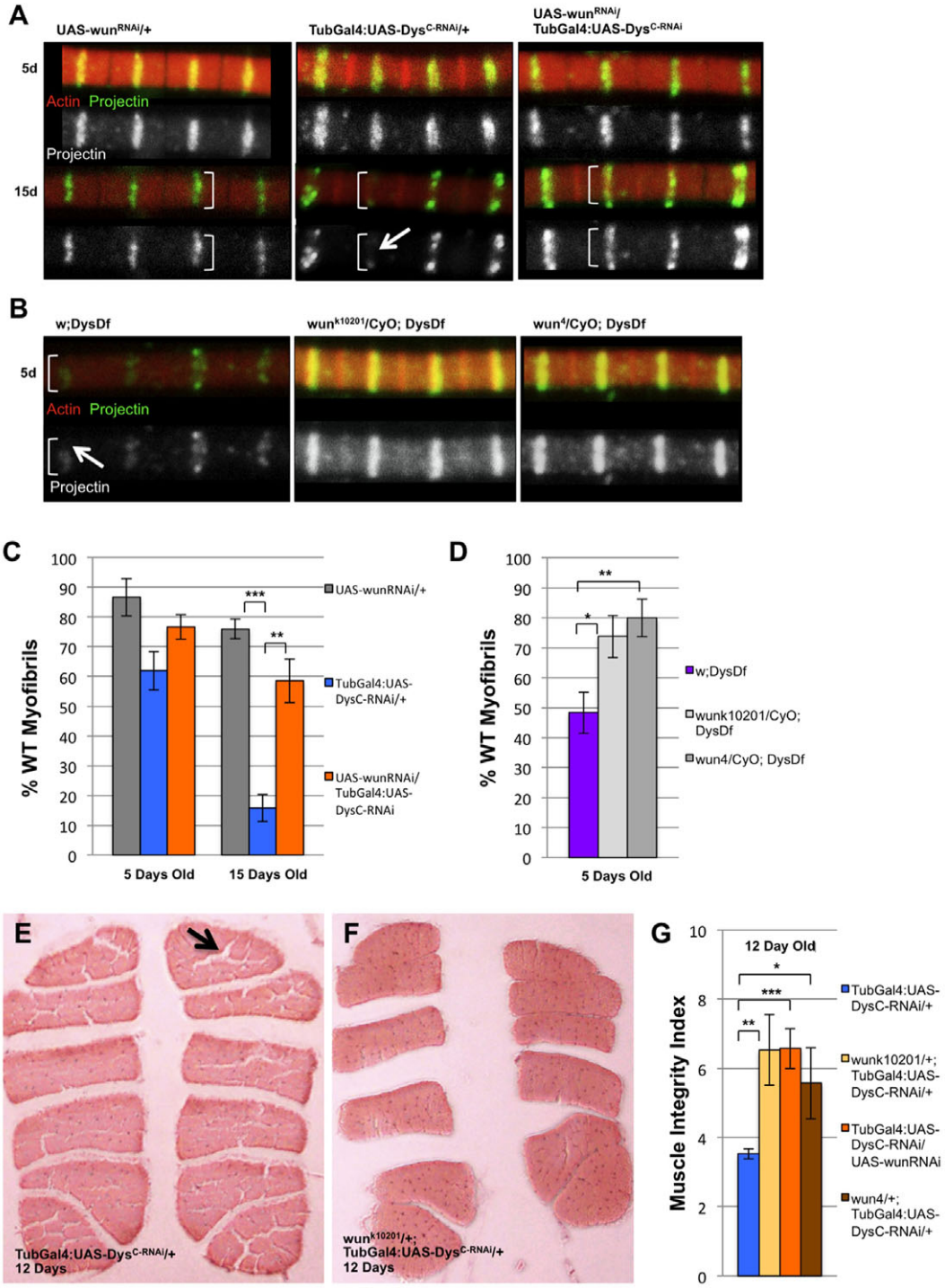

Fig. 2. Dystrophic flies with reduced *wunen* have less age-dependent degeneration over time. (**A**) Confocal images of individual IFM myofibrils of 5- and 15-day-old flies of the following genotypes (from left to right): undriven *UAS-wun^{RNAi}*/+, tubulin-Gal4-driven *Dys* RNAi (*TubGal4:UAS-Dys$^{C\text{-}RNAi}$*/+) and tubulin-Gal4-driven *wun* RNAi, *Dys* RNAi double knockdown (*UAS-wun^{RNAi}/TubGal4:UAS-Dys$^{C\text{-}RNAi}$*). (**B**) Confocal images of individual IFM myofibrils of 5-day-old flies of the following genotypes (from left to right): *w;DysDf* and the same *Dys* mutant with reduced *wunen* (*wun^{k10201}* and *wun^{4}*). (**C**) Percentage of wild-type IFM myofibrils from each genotype shown in A at 5 and 15 days including UAS-wunRNAi/+, tubulin-Gal4-driven *Dys* RNAi (*TubGal4:UAS-Dys$^{C\text{-}RNAi}$*/+) and tubulin-Gal4-driven *wun* RNAi in *Dys* RNAi background (*UAS-wun^{RNAi}/TubGal4:UAS-Dys$^{C\text{-}RNAi}$*). (**D**) Percentage of wild-type IFM myofibrils from each genotype shown in B at 5 days. (**E**) Tubulin-Gal4-driven *Dys* RNAi mutant transverse section (H&E stained) from a 12-day-old fly. Black arrow shows a hole in the flight muscle indicative of severe degeneration. (**F**) Transverse section (H&E stained) of a 12-day-old tubulin-Gal4-driven *Dys* RNAi mutant with reduced *wunen* (*wun^{k10201}*) in the background. At least nine flies of each genotype were used per experiment. Each experiment was repeated three times. (**G**) Muscle integrity index of the tubulin-Gal4-driven *Dys* RNAi mutant alone and with reduced *wunen* (*wun^{k10201}*, *wun^{RNAi}*, *wun^{4}*). In A and B, white brackets indicate width of the myofibril; white arrows indicate a representative defective Projectin pattern; Actin (red) and Projectin (green, grayscale). *P<0.05, **P<0.01, ***P<0.001. Error bars represent s.e.m.

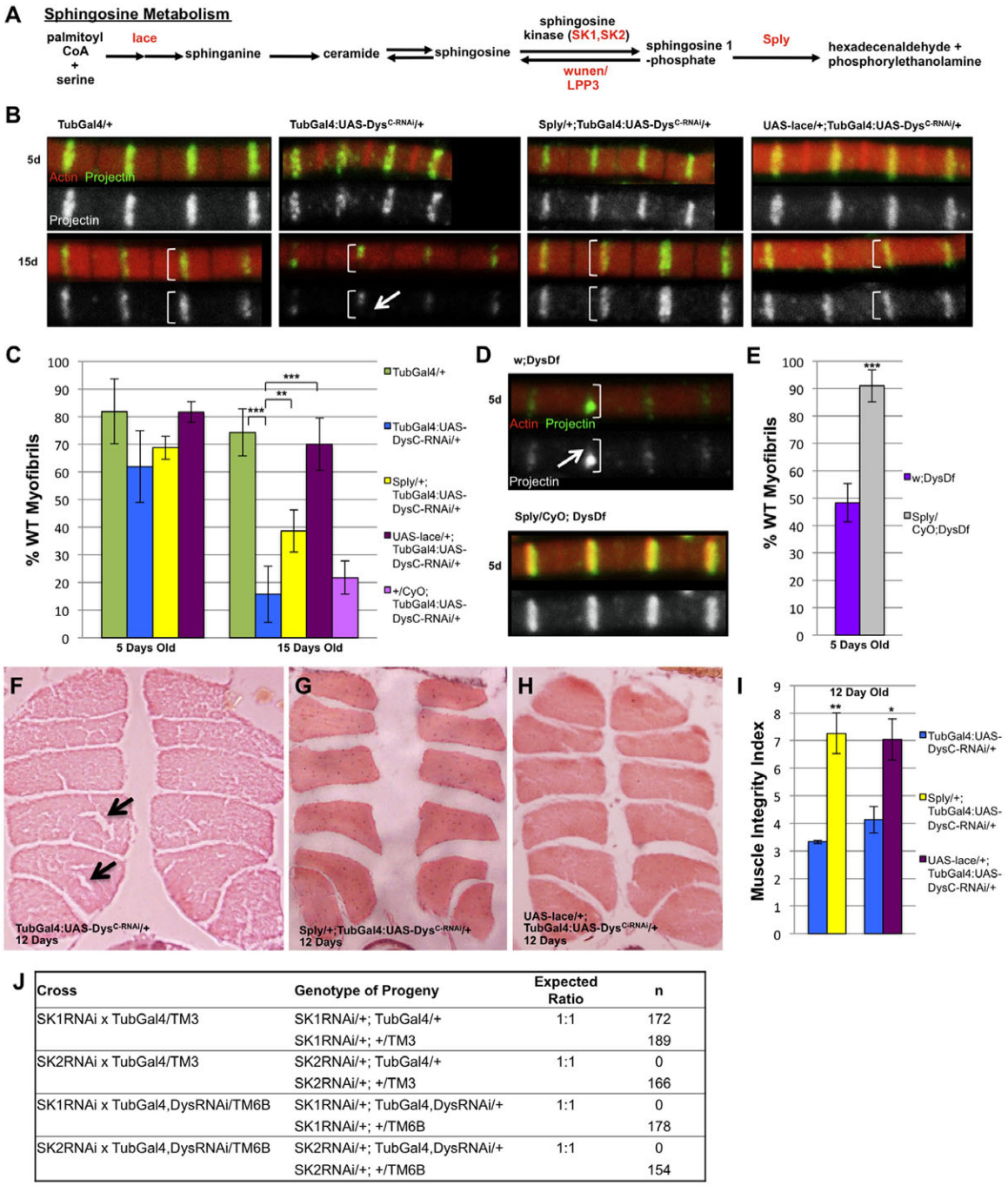

J

Cross	Genotype of Progeny	Expected Ratio	n
SK1RNAi x TubGal4/TM3	SK1RNAi/+; TubGal4/+	1:1	172
	SK1RNAi/+; +/TM3		189
SK2RNAi x TubGal4/TM3	SK2RNAi/+; TubGal4/+	1:1	0
	SK2RNAi/+; +/TM3		166
SK1RNAi x TubGal4,DysRNAi/TM6B	SK1RNAi/+; TubGal4,DysRNAi/+	1:1	0
	SK1RNAi/+; +/TM6B		178
SK2RNAi x TubGal4,DysRNAi/TM6B	SK2RNAi/+; TubGal4,DysRNAi/+	1:1	0
	SK2RNAi/+; +/TM6B		154

Fig. 3. Dystrophic muscle phenotypes are suppressed with altered sphingolipid metabolism gene dosage. (**A**) *De novo* sphingolipid synthesis pathway. (**B**) Confocal images of individual IFM myofibrils of 5- and 15-day-old flies of the following genotypes (from left to right): tubulin-Gal4 (*TubGal4*/+), tubulin-Gal4-driven *Dys* RNAi (*TubGal4:UAS-Dys*$^{C\text{-}RNAi}$/+), *Sply*, *Dys* double heterozygote (*Sply*/+*; TubGal4:UAS-Dys*$^{C\text{-}RNAi}$/+), and the *Dys* mutant with overexpressed *lace* (*UAS-lace*/+*;TubGal4:UAS-Dys*$^{C\text{-}RNAi}$/+). Actin (red) and Projectin (green, grayscale). White brackets indicate width of the myofibril. White arrows indicate a representative defective Projectin pattern. (**C**) Percentage of wild-type IFM myofibrils from each genotype shown in B at 5 and 15 days as well as from flies with tubulin-Gal4-driven *Dys* RNAi with the second chromosome balancer CyO (*+/CyO;TubGal4:UAS-Dys*$^{C\text{-}RNAi}$/+). (**D**) Confocal images of individual IFM myofibrils of 5-day-old flies of the following genotypes: *w*;*DysDf* and *w*; *Sply*/+*; DysDf*. (**E**) Graph quantifying the percentage of wild-type IFM myofibrils from each genotype shown in D at 5 days. (**F**) Transverse section (H&E stained) of a tubulin-Gal4-driven *Dys* RNAi 12-day-old mutant fly (*TubGal4:UAS-Dys*$^{C\text{-}RNAi}$/+). Black arrows indicate holes in the flight muscle indicative of the most severe degeneration. (**G**) Transverse section (H&E stained) of a tubulin-Gal4-driven *Dys* RNAi 12-day-old mutant with reduced *Sply* (*Sply*/+*; TubGal4:UAS-Dys*$^{C\text{-}RNAi}$/+). (**H**) Transverse section (H&E stained) of a tubulin-Gal4-driven *Dys* RNAi 12-day-old mutant with *lace* overexpressed (*UAS-lace*/+*;TubGal4:UAS-Dys*$^{C\text{-}RNAi}$/+). (**I**) Graph comparing the muscle integrity index of the tubulin-Gal4-driven *Dys* RNAi mutant alone (*TubGal4:UAS-Dys*$^{C\text{-}RNAi}$/+), with reduced *Sply* (*Sply*/+*; TubGal4:UAS-Dys*$^{C\text{-}RNAi}$/+), and with overexpressed *lace* (*UAS-lace*/+*;TubGal4:UAS-Dys*$^{C\text{-}RNAi}$/+). Eight flies were sectioned per experiment; each experiment was repeated three times; total *n*=24 for each genotype. (**J**) Table of viability of globally reducing the sphingosine kinases (SK1 and SK2) by expressing RNAi transgenes using the tubulin-Gal4 driver in the presence and absence of *Dys* RNAi. ***P*<0.01, ****P*<0.001. Error bars represent s.e.m.

system (Fig. 5A; Materials and methods). Using this system we show that the overall activity of dystrophic flies of genotypes *w; DysDf/DysDf*, *w; Dys^{det1}/Dys^{det1}* and *w; Dys$^{C\text{-}RNAi}$/+* when measured continuously over 6, 2 and 3 days, respectively, is significantly lowered compared with control *w* flies (Fig. 5B,C; supplementary material Fig. S1F). Activity of dystrophic flies was generally 50% lower than non-dystrophic control flies when tested over different durations of time.

To assess muscle function in dystrophic flies with reduced *wunen*, we used both the automated activity monitoring system and the countercurrent climbing apparatus. We generated animals with the single chromosome *Dystrophin* RNAi mutations that we had previously generated [*TubGal4:UAS-Dys$^{C\text{-}RNAi}$* described above and *ActGal4:UAS-Dys$^{N\text{-}RNAi}$* (Kucherenko et al., 2008)] combined with several *wunen* alleles (*wun^{k10201}*, *wun^{RNAi}* and *wun^{4}*) to determine whether there was a suppression of dystrophic muscle function. Fig. 5D shows that all combinations of the *Dystrophin* mutants with different *wunen* alleles markedly increased activity compared with the *Dystrophin* mutants alone. Briefly, over the course of three days, 15-day-old dystrophic flies with reduced *wunen* were significantly more active (approximately twofold higher) than dystrophic flies alone. This correlated with the climbing analysis performed with the tubulin-Gal4 *Dys$^{C\text{-}RNAi}$* dystrophic animals with the *wunen* alleles mentioned above. This analysis showed that reduced *wunen* significantly increased the climbing ability of dystrophic flies (Fig. 5D). Additionally, we found that a viable 15-day-old *wunen* mutant alone (*wun^{EY11935}*) was significantly more active than wild-type (*OR*) flies. At this age, we see significant lethality with *Dys^{det1}* mutant flies (supplementary material Fig. S2).

As with the suppression of the physical muscle defects described above, we investigated whether the genetic elevation of S1P through the reduction of *Sply* and overexpression of *lace* would manifest as increased activity in dystrophic animals. As with the muscle structural analysis, we again used the tubulin-Gal4-driven RNAi dystrophic animals to assess activity with reduced *Sply*. Automated monitoring analysis revealed a significant increase in activity when *Sply* was reduced in 12-day-old dystrophic flies (Fig. 5F). For the *lace* overexpression studies, we used both RNAi dystrophic animals (*TubGal4:UAS-Dys$^{C\text{-}RNAi}$* and *ActGal4:UAS-Dys$^{N\text{-}RNAi}$*) with *UAS-lace* in the background and found that with the transgene present 15-day-old dystrophic flies were significantly more active than flies without *lace* overexpression (Fig. 5G).

Finally, to determine whether reduction of *spinster* expression in dystrophic flies would also yield more active flies, we assayed 7-day-old flies and found that, like the S1P metabolism genes used above, dystrophic flies heterozygous for a strong *spin* allele showed a nearly twofold increase in activity (Fig. 5H).

Suppression of dystrophic muscle phenotypes using pharmacological agents that increase S1P levels or S1P signaling

In rodents, the genetic reduction of S1P lyase activity can be phenocopied pharmacologically by the delivery of the small molecule 2-acetyl-4(5)-tetrahydroxybutyl imidazole (THI) (Fig. 6F) (Schwab et al., 2005; Bagdanoff et al., 2009). We determined whether this small molecule would have the same effect in *Drosophila* by testing whether dystrophic mutant flies of differing genotypes (*TubGal4:UAS-Dys$^{C\text{-}RNAi}$/+*, an RNAi knockdown mutant; *Dys^{det1}*, a hypomorph; *DysDf*, a *Dystrophin* deficiency mutant; and *Dys^{det1}/DysDf*) given food supplemented with THI would show any suppression of the muscle degeneration phenotypes. After 3 days on a feeding regimen with THI (Fig. 6A), myofibrils from 7- to 10-day-old flies were harvested and analyzed, revealing a significant suppression of muscle wasting in dystrophic flies of all genotypes tested (Fig. 6B,C,E). Longer treatment also appears to be beneficial as after a 14-day feeding regimen we observe similar muscle wasting suppression in myofibrils from 15-day-old flies (supplementary material Fig. S3A,B). Even further suppression was observed when the feeding regimen of THI was combined with genetically reduced *Sply* (Fig. 6B; *Sply/+; TubGal4:UAS-Dys$^{C\text{-}RNAi}$/+* with THI). Note that the flies with genetically reduced *Sply* that were not fed food supplemented with THI had more intact myofibrils, which is consistent with elevated S1P suppressing muscle wasting. In addition to muscle wasting suppression, we observe a functional benefit when feeding dystrophic flies food supplemented with THI. The activity

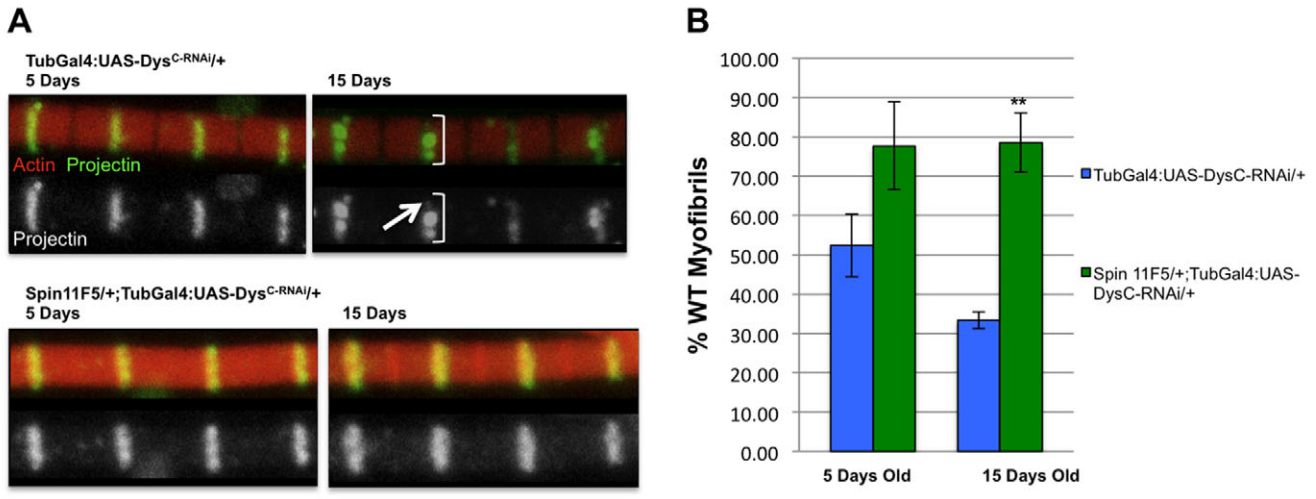

Fig. 4. Suppression of the dystrophic myofibril phenotype by genetic reduction of Spinster, a putative S1P transporter. (**A**) Confocal images of individual IFM myofibrils of 5- and 15-day-old flies of the following genotypes: tubulin-Gal4-driven *Dys* RNAi (*TubGal4:UAS-Dys$^{C\text{-}RNAi}$/+*) and the *spin^{11F5}*, *Dys* double heterozygote (*spin^{11F5}/+; TubGal4:UAS-Dys$^{C\text{-}RNAi}$/+*). Actin (red) and Projectin (green, grayscale). White brackets indicate width of the myofibril. Arrow indicates a representative defective Projectin pattern. (**B**) Percentage of wild-type IFM myofibrils from each genotype shown in A at 5 and 15 days. $^{**}P<0.01$. Error bars represent s.e.m.

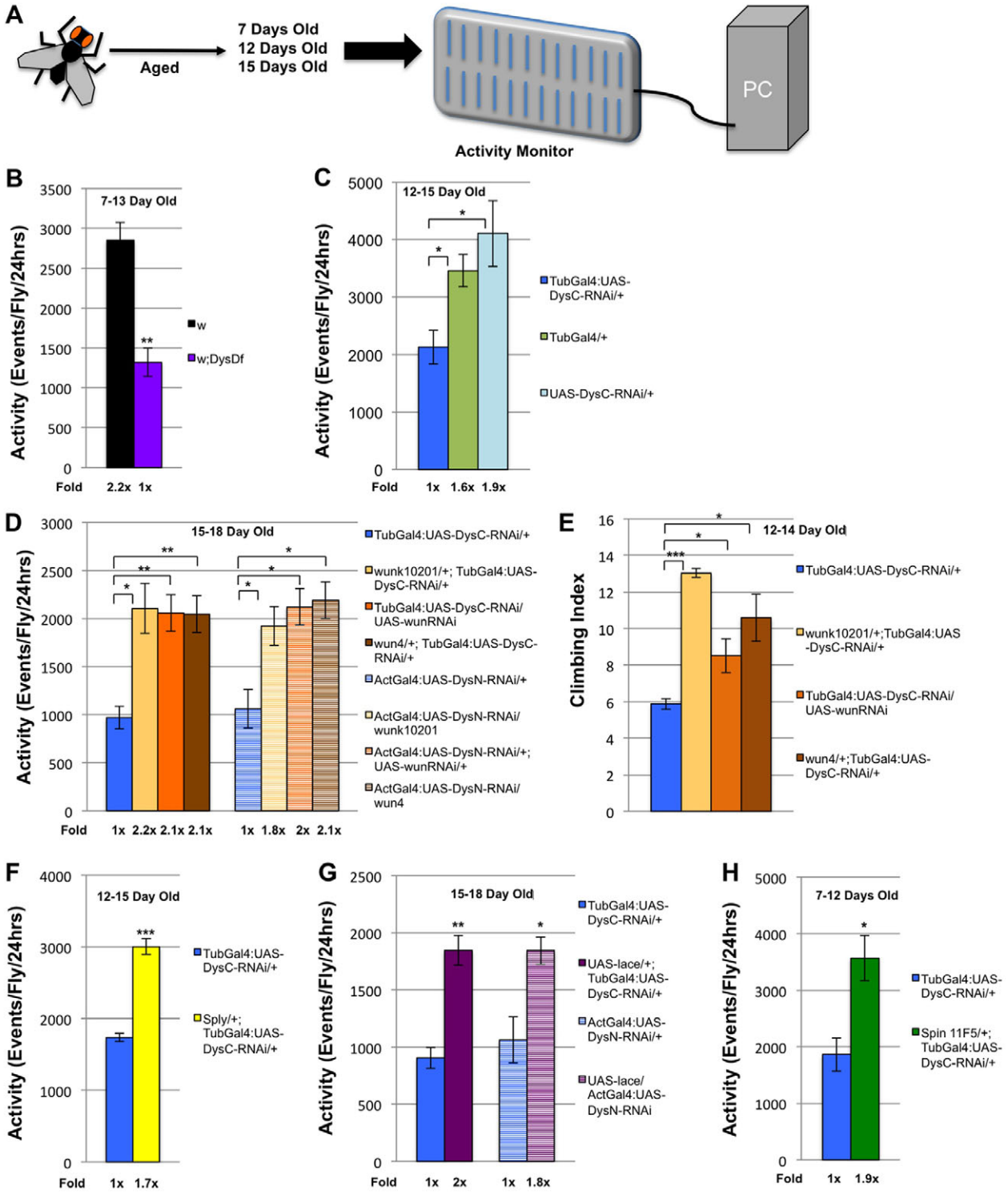

Fig. 5. Dystrophic movement phenotypes suppressed with genetic elevation of S1P. (**A**) Experimental flow for automated activity monitoring. (**B**) Activity analysis of 7-day-old *w;DysDf* and *w* control flies over 144 hours. (**C**) Activity analysis of 12-day-old tubulin-Gal4-driven *Dys* RNAi mutant and transgene control flies *TubGal4/+* and *UAS-Dys*$^{C\text{-}RNAi}$*/+* monitored over 72 hours. (**D**) Activity analysis of 15-day-old tubulin- or actin-Gal4-driven *Dys* RNAi mutants alone and combined with different *wunen* alleles (*wun*^{k10201}, *wun*^{RNAi}, *wun*^{4}) over 72 hours. (**E**) Climbing index comparing 12- to 14-day-old dystrophic flies (*TubGal4:UAS-Dys*$^{C\text{-}RNAi}$*/+*) alone and with reduced *wunen* (*wun*^{k10201}, *wun*^{RNAi}, *wun*^{4}). Twenty flies were used per experiment; each experiment was repeated three times. (**F**) Activity analysis of the 12-day-old tubulin-Gal4-driven *Dys* RNAi (*TubGal4:UAS-Dys*$^{C\text{-}RNAi}$*/+*) mutant alone and with reduced *Sply* (*Sply/+; TubGal4:UAS-Dys*$^{C\text{-}RNAi}$*/+*). (**G**) Activity analyses of 15-day-old tubulin- and actin-Gal4 *Dys* RNAi mutants alone and with overexpressed *lace* (*TubGal4:UAS-Dys*$^{C\text{-}RNAi}$*/+*, *UAS-lace/+;TubGal4:UAS-Dys*$^{C\text{-}RNAi}$*/+*, and *ActGal4:UAS-Dys*$^{N\text{-}RNAi}$*/+* and *UAS-lace/ActGal4:UAS-Dys*$^{N\text{-}RNAi}$). (**H**) Activity analysis of the 7-day-old tubulin-Gal4-driven *Dys* RNAi (*TubGal4:UAS-Dys*$^{C\text{-}RNAi}$*/+*) mutant alone and with reduced *spin* (*spin*^{11F5}*/+; TubGal4:UAS-Dys*$^{C\text{-}RNAi}$*/+*). *P<0.05, **P<0.01, ***P<0.001. Error bars represent s.e.m.

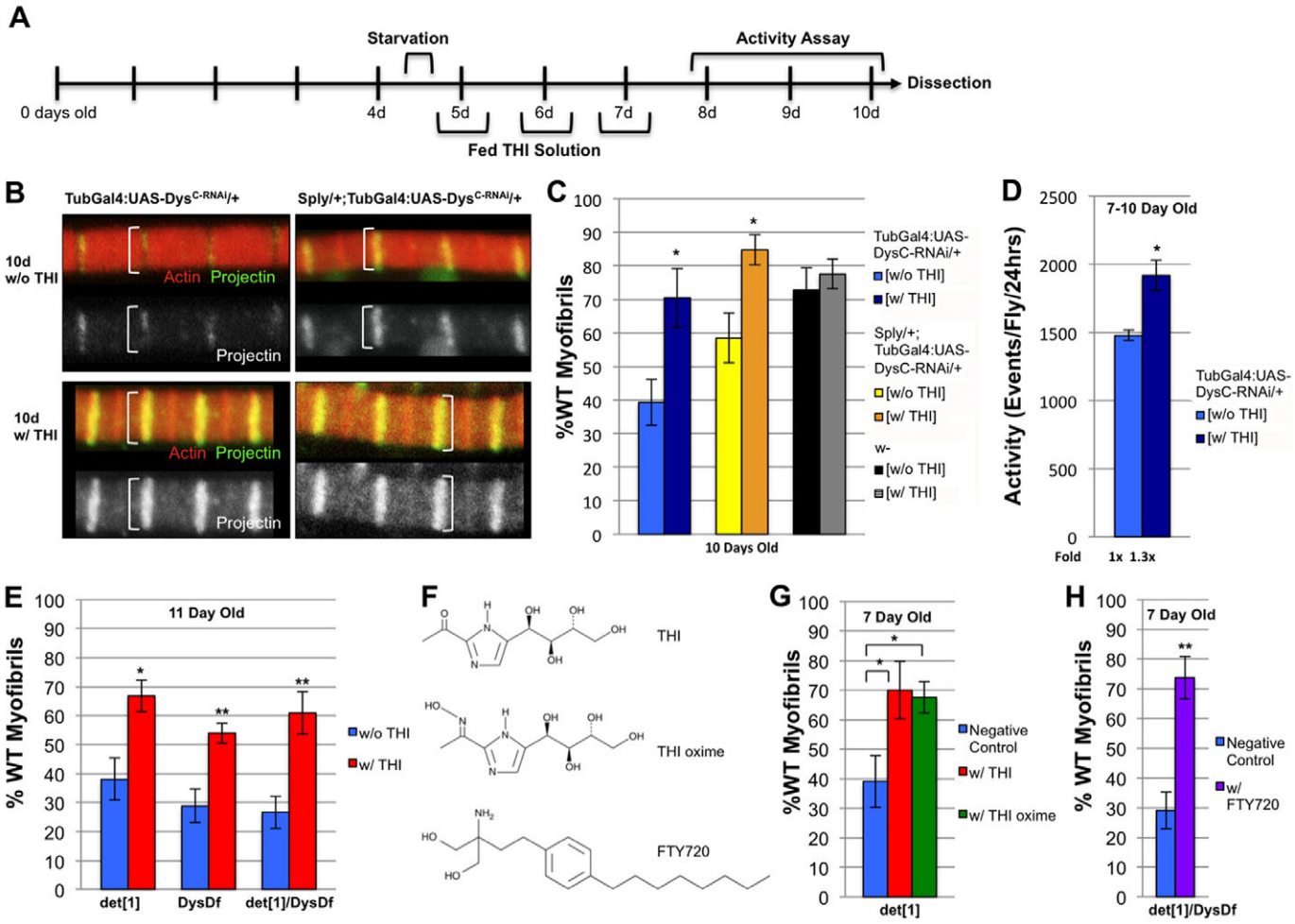

Fig. 6. Dystrophic phenotypes suppressed with THI treatment during adulthood. (**A**) Experimental timeline of THI administration to *Drosophila*. (**B**) Confocal images of individual IFM myofibrils isolated at 10 days of tubulin-Gal4-driven *Dys* RNAi (*TubGal4:UAS-Dys$^{C\text{-}RNAi}$/+*) mutants alone and with reduced *Sply* (*Sply/+; TubGal4:UAS-Dys$^{C\text{-}RNAi}$/+*) that were fed a corn syrup solution with and without THI. Actin (red) and Projectin (green, grayscale). White brackets indicate the width of the myofibril. Arrow indicates reduction/loss of Projectin staining at the Z-band. (**C**) Percentage of wild-type myofibrils from tubulin-Gal4-driven *Dys* RNAi (*TubGal4:UAS-Dys$^{C\text{-}RNAi}$/+*), *Sply*, *Dys* double heterozygote (*Sply/+; TubGal4:UAS-Dys$^{C\text{-}RNAi}$/+*) flies fed a corn syrup solution with and without THI. (**D**) Activity analysis of tubulin-Gal4-driven *Dys* RNAi (*TubGal4:UAS-Dys$^{C\text{-}RNAi}$/+*) flies fed a corn syrup solution with and without THI. (**E**) Percentage of wild-type myofibrils from 11-day-old *Dys* mutants (*Dys^{det1}*, *DysDf* and *Dys^{det1}/DysDf*) fed a corn syrup solution with and without THI. (**F**) Chemical structures of THI, THI oxime and FTY720. (**G**) Percentage of wild-type myofibrils from 7-day-old *Dys^{det1}* flies fed a corn syrup solution with and without THI and THI oxime. (**H**) Percentage of wild-type myofibrils from 7-day-old *Dys^{det1}/DysDf* flies fed a corn syrup solution with and without FTY720. For activity assays, six flies of each genotype listed on the *x*-axis were analyzed per experiment; each experiment was repeated three times. Total time per experiment was 72 hours; total n=18. *P<0.05. Error bars represent s.e.m.

analysis revealed that dystrophic flies fed solutions supplemented with THI were significantly more active than flies fed solutions not supplemented with THI (Fig. 6D).

To determine whether other small molecules, particularly drugs that either increase S1P levels or S1P signaling, would produce similar results to THI, we tested THI oxime (Fig. 6F), a candidate for the treatment of rheumatoid arthritis (Bagdanoff et al., 2010). As THI oxime is a derivative of THI we expected and found their beneficial effects to be similar in dystrophic muscles. Myofibrils isolated from 7-day-old *Dys^{det1}* mutant flies after 3 days of THI oxime treatment showed significant suppression of Projectin disruption (Fig. 6G). Finally, we tested FTY720, an analog of S1P and potent elevator of S1P signaling (Napoli, 2000; Bagdanoff et al., 2009; Bagdanoff et al., 2010), for its effect on muscle wasting when fed to *Dys^{det1}/DysDf* flies. Using the same 3-day treatment, myofibrils isolated from 7-day-old flies revealed very strong suppression of the myofibril degeneration phenotype (Fig. 6H).

DISCUSSION

Here, we have established an easy-to-score myofibril phenotype for dystrophic flies that can even be scored in relatively young flies in strong *Dystrophin* mutants (Fig. 1). This assay complements the histological sections used previously to score gross morphological muscle degeneration. In using both assays, we have shown that a reduction of the LPP3 homolog *wunen* prevents, to a significant degree, Dystrophin-dependent muscle wasting (Fig. 2). Our data suggest that this is likely to occur through the increase of S1P levels as other avenues used to raise the level of S1P phenocopied this suppression. Both reduction of *Sply*, encoding the *Drosophila*

S1P lyase, and overexpression of *lace*, encoding the catalytic subunit of serine palmitoyl CoA transferase in the *de novo* sphingolipid synthesis pathway, prevent muscle wasting (Fig. 3). We have also shown that muscle function as assayed by fly movement is also improved in dystrophic animals when S1P is genetically elevated (Fig. 5). Furthermore, we have shown that S1P-based suppression is not occurring during development as feeding experiments utilizing adult flies have revealed that S1P elevation in these animals can suppress dystrophic myofibril and activity phenotypes (Fig. 6)

Our data also suggest that minimal levels of S1P are necessary for viability in *Drosophila* as global reduction of Sphingosine Kinase 2 (SK2) results in lethality. Interestingly, global reduction of Sphingosine Kinase 1 (SK1) is not lethal in non-dystrophic flies yet is lethal in dystrophic flies (Fig. 3J), owing to exacerbation of the phenotype. These data indicate that S1P levels regulated by SK1 are crucial for *Dystrophin* mutant survival. These data argue for a precise requirement of minimal levels of S1P for muscle development and/or function. Future analyses of the activity of both sphingosine kinases in different tissues and cellular compartments might separate the roles of each kinase in homeostasis and muscle.

In mammals, there are five S1P receptors that share homology with G protein-coupled receptors (Rosen et al., 2009). Though flies do have G protein-coupled receptors, they do not appear to have the S1P receptors seen in vertebrates, suggesting that S1P receptor-mediated signaling might have evolved later in higher organisms. S1P lyase mutants increase intracellular S1P levels (Ikeda et al., 2004) and S1P is generated and has been shown to function inside the cells (Hait et al., 2009; Breslow and Weissman, 2010; Strub et al., 2010; Yonamine et al., 2011), indicating that the suppression of muscle wasting in *Drosophila* occurs intracellularly. With this in mind, we hypothesized that if *spinster*, like its mammalian homolog *spns2*, were an S1P transporter its reduction would prevent S1P from leaving the cytoplasmic compartment and it would then behave like reduced *Sply* and suppress muscle wasting. Our data support this hypothesis (Fig. 4) yet more work is required to connect this transporter to S1P in *Drosophila*. Interestingly, *Drosophila spinster* has been reported to interact with genes of the cell death pathway (Sakurai et al., 2010) and it is known that ceramide in the sphingolipid pathway can induce cell death. Perhaps *spinster* alters the cell death pathway by perturbing the equilibrium of sphingolipids, particularly S1P, in different subcellular compartments. A recent report has revealed S1P epigenetic regulation of gene expression through direct intracellular interaction with histone deacetylases (HDACs) (Hait et al., 2009). Through this mechanism, perhaps increasing intracellular S1P levels alters gene expression, which ultimately leads to elevated translation of muscle proteins, such as Projectin, which then reduces muscle wasting.

As mentioned, S1P has been shown to be necessary for the proliferation of satellite cells in mammals and is required for differentiation of myoblasts to myotubes (Bruni and Donati, 2008). As there do not appear to be canonical satellite cells in *Drosophila*, i.e. muscle precursor cells located on the surface of muscle fibers, perhaps S1P-based suppression of muscle wasting occurs as a result of the requirement of S1P for proper differentiation. It has been reported in *Drosophila* that sarcomeres are formed by an assembly of latent protein complexes (Rui et al., 2010). It would be consistent with this if S1P elevates muscle protein synthesis (in turn increasing the level of latent protein complexes) so that after muscle contraction-induced damage these complexes can assemble and produce new myofibrils. Our work with small molecule effectors of S1P signaling indicate that the abovementioned possibilities for suppression occur in actively contracting adult muscle.

S1P-based suppression of muscle wasting can be dissected further in *Drosophila* with the abundance of genetic tools available. Furthermore, given our results with THI, THI oxime and FTY720, *Drosophila* may be used to screen small molecules for their efficacy in suppressing muscle wasting.

Acknowledgements
We thank members of the Ruohola-Baker laboratory and Prof. Guenter Daum for helpful discussions throughout this work. We thank Prof. Leo Pallanck and Dr Susan McNabb for providing the climbing and activity apparatuses. We also thank Dr Andriy Buchynskyy and Prof. Michael Gelb for THI oxime.

Funding
This work was supported by the National Institutes of Health (NIH) American Recovery and Reinvestment Act (ARRA) Challenge Grant [5RC1AR058520 to H.R.-B.]. This work was also partly supported by NIH grants [R01GN06278, R01GM083867, R01GM097372 and 1P01GM081619 to H.R.-B.]. Support was also received from the University of Washington Nathan Shock Center of Excellence in the Basic Biology of Aging, Genetic Approaches to Aging Training Grant [T32 AG00057 to N.I.]; and from the Duchenne Alliance, RaceMD and Ryan's Quest [to M.P., N.I., M.R. and H.R.-B.]. Deposited in PMC for release after 12 months.

Competing interests statement
The authors declare no competing financial interests.

Supplementary material
Supplementary material available online at
http://dev.biologists.org/lookup/suppl/doi:10.1242/dev.087791/-/DC1

References

Adachi-Yamada, T., Gotoh, T., Sugimura, I., Tateno, M., Nishida, Y., Onuki, T. and Date, H. (1999). De novo synthesis of sphingolipids is required for cell survival by down-regulating c-Jun N-terminal kinase in Drosophila imaginal discs. *Mol. Cell. Biol.* **19**, 7276-7286.

Ayme-Southgate, A., Saide, J., Southgate, R., Bounaix, C., Cammarato, A., Patel, S. and Wussler, C. (2005). In indirect flight muscles Drosophila projectin has a short PEVK domain, and its NH2-terminus is embedded at the Z-band. *J. Muscle Res. Cell Motil.* **26**, 467-477.

Bagdanoff, J. T., Donoviel, M. S., Nouraldeen, A., Tarver, J., Fu, Q., Carlsen, M., Jessop, T. C., Zhang, H., Hazelwood, J., Nguyen, H. et al. (2009). Inhibition of sphingosine-1-phosphate lyase for the treatment of autoimmune disorders. *J. Med. Chem.* **52**, 3941-3953.

Bagdanoff, J. T., Donoviel, M. S., Nouraldeen, A., Carlsen, M., Jessop, T. C., Tarver, J., Aleem, S., Dong, L., Zhang, H., Boteju, L. et al. (2010). Inhibition of sphingosine 1-phosphate lyase for the treatment of rheumatoid arthritis: discovery of (E)-1-(4-((1R,2S,3R)-1,2,3,4-tetrahydroxybutyl)-1H-imidazol-2-yl)ethanone oxime (LX2931) and (1R,2S,3R)-1-(2-(isoxazol-3-yl)-1H-imidazol-4-yl)butane-1,2,3,4-tetraol (LX2932). *J. Med. Chem.* **53**, 8650-8662.

Benzer, S. (1967). Behavioural mutants of Drosophila isolated by countercurrent distribution. *Proc. Natl. Acad. Sci. USA* **58**, 1112-1119.

Breslow, D. K. and Weissman, J. S. (2010). Membranes in balance: mechanisms of sphingolipid homeostasis. *Mol. Cell* **40**, 267-279.

Brindley, D. N. and Pilquil, C. (2009). Lipid phosphate phosphatases and signaling. *J. Lipid Res.* **50**, S225-S230.

Bruni, P. and Donati, C. (2008). Pleiotropic effects of sphingolipids in skeletal muscle. *Cell. Mol. Life Sci.* **65**, 3725-3736.

Bullard, B., Garcia, T., Benes, V., Leake, M. C., Linke, W. A. and Oberhauser, A. F. (2006). The molecular elasticity of the insect flight muscle proteins projectin and kettin. *Proc. Natl. Acad. Sci. USA* **103**, 4451-4456.

Burnett, C. and Howard, K. (2003). Fly and mammalian lipid phosphate phosphatase isoforms differ in activity both in vitro and in vivo. *EMBO Rep.* **4**, 793-799.

Christoforou, C. P., Greer, C. E., Challoner, B. R., Charizanos, D. and Ray, R. P. (2008). The detached locus encodes Drosophila Dystrophin, which acts with other components of the Dystrophin Associated Protein Complex to influence intercellular signalling in developing wing veins. *Dev. Biol.* **313**, 519-532.

Collins, C. A. and Morgan, J. E. (2003). Duchenne's muscular dystrophy: animal models used to investigate pathogenesis and develop therapeutic strategies. *Int. J. Exp. Pathol.* **84**, 165-172.

Deconinck, N. and Dan, B. (2007). Pathophysiology of duchenne muscular dystrophy: current hypotheses. *Pediatr. Neurol.* **36**, 1-7.
Dietzl, G., Chen, D., Schnorrer, F., Su, K.-C., Barinova, Y., Fellner, M., Gasser, B., Kinsey, K., Oppel, S., Scheiblauer, S. et al. (2007). A genome-wide transgenic RNAi library for conditional gene inactivation in Drosophila. *Nature* **448**, 151-156.
Greene, J. C., Whitworth, A. J., Kuo, I., Andrews, L. A., Feany, M. B. and Pallanck, L. J. (2003). Mitochondrial pathology and apoptotic muscle degeneration in Drosophila parkin mutants. *Proc. Natl. Acad. Sci. USA* **100**, 4078-4083.
Hackman, P., Vihola, A., Haravuori, H., Marchand, S., Sarparanta, J., De Seze, J., Labeit, S., Witt, C., Peltonen, L., Richard, I. et al. (2002). Tibial muscular dystrophy is a titinopathy caused by mutations in TTN, the gene encoding the giant skeletal-muscle protein titin. *Am. J. Hum. Genet.* **71**, 492-500.
Hait, N. C., Allegood, J., Maceyka, M., Strub, G. M., Harikumar, K. B., Singh, S. K., Luo, C., Marmorstein, R., Kordula, T., Milstien, S. et al. (2009). Regulation of histone acetylation in the nucleus by sphingosine-1-phosphate. *Science* **325**, 1254-1257.
Hisano, Y., Kobayashi, N., Kawahara, A., Yamaguchi, A. and Nishi, T. (2011). The sphingosine 1-phosphate transporter, SPNS2, functions as a transporter of the phosphorylated form of the immunomodulating agent FTY720. *J. Biol. Chem.* **286**, 1758-1766.
Ikeda, M., Kihara, A. and Igarashi, Y. (2004). Sphingosine-1-phosphate lyase SPL is an endoplasmic reticulum-resident, integral membrane protein with the pyridoxal 5′-phosphate binding domain exposed to the cytosol. *Biochem. Biophys. Res. Commun.* **325**, 338-343.
Kawahara, A., Nishi, T., Hisano, Y., Fukui, H., Yamaguchi, A. and Mochizuki, N. (2009). The sphingolipid transporter spns2 functions in migration of zebrafish myocardial precursors. *Science* **323**, 524-527.
Kucherenko, M. M., Pantoja, M., Yatsenko, A. S., Shcherbata, H. R., Fischer, K. A., Maksymiv, D. V., Chernyk, Y. I. and Ruohola-Baker, H. (2008). Genetic modifier screens reveal new components that interact with the Drosophila dystroglycan-dystrophin complex. *PLoS ONE* **3**, e2418.
Lakey, A., Ferguson, C., Labeit, S., Reedy, M., Larkins, A., Butcher, G., Leonard, K. and Bullard, B. (1990). Identification and localization of high molecular weight proteins in insect flight and leg muscle. *EMBO J.* **9**, 3459-3467.
Long, J., Darroch, P., Wan, K. F., Kong, K. C., Ktistakis, N., Pyne, N. J. and Pyne, S. (2005). Regulation of cell survival by lipid phosphate phosphatases involves the modulation of intracellular phosphatidic acid and sphingosine 1-phosphate pools. *Biochem. J.* **391**, 25-32.
Matsumura, K., Shimizu, T., Nonaka, I. and Mannen, T. (1989). Immunochemical study of connectin (titin) in neuromuscular diseases using a monoclonal antibody: connectin is degraded extensively in Duchenne muscular dystrophy. *J. Neurol. Sci.* **93**, 147-156.
Mendell, J. R., Rodino-Klapac, L. R. and Malik, V. (2010). Molecular therapeutic strategies targeting Duchenne muscular dystrophy. *J. Child Neurol.* **25**, 1145-1148.
Moore, J. R., Vigoreaux, J. O. and Maughan, D. W. (1999). The Drosophila projectin mutant, bentD, has reduced stretch activation and altered indirect flight muscle kinetics. *J. Muscle Res. Cell Motil.* **20**, 797-806.
Nagata, Y., Partridge, T. A., Matsuda, R. and Zammit, P. S. (2006). Entry of muscle satellite cells into the cell cycle requires sphingolipid signaling. *J. Cell Biol.* **174**, 245-253.
Napoli, K. L. (2000). The FTY720 story. *Ther. Drug Monit.* **22**, 47-51.
Osborne, N., Brand-Arzamendi, K., Ober, E. A., Jin, S.-W., Verkade, H., Holtzman, N. G., Yelon, D. and Stainier, D. Y. R. (2008). The spinster homolog, two of hearts, is required for sphingosine 1-phosphate signaling in zebrafish. *Curr. Biol.* **18**, 1882-1888.
Palmieri, B., Tremblay, J. P. and Daniele, L. (2010). Past, present and future of myoblast transplantation in the treatment of Duchenne muscular dystrophy. *Pediatr. Transplant.* **14**, 813-819.
Perkins, A. D., Ellis, S. J., Asghari, P., Shamsian, A., Moore, E. D. W. and Tanentzapf, G. (2010). Integrin-mediated adhesion maintains sarcomeric integrity. *Dev. Biol.* **338**, 15-27.
Pyne, S., Long, J. S., Ktistakis, N. T. and Pyne, N. J. (2005). Lipid phosphate phosphatases and lipid phosphate signalling. *Biochem. Soc. Trans.* **33**, 1370-1374.
Rapizzi, E., Donati, C., Cencetti, F., Nincheri, P. and Bruni, P. (2008). Sphingosine 1-phosphate differentially regulates proliferation of C2C12 reserve cells and myoblasts. *Mol. Cell. Biochem.* **314**, 193-199.
Rosen, H., Gonzalez-Cabrera, P. J., Sanna, M. G. and Brown, S. (2009). Sphingosine 1-Phosphate Receptor Signaling. *Annu. Rev. Biochem.* **78**, 743-768.
Rui, Y., Bai, J. and Perrimon, N. (2010). Sarcomere formation occurs by the assembly of multiple latent protein complexes. *PLoS Genet.* **6**, e1001208.
Sakurai, A., Nakano, Y., Koganezawa, M. and Yamamoto, D. (2010). Phenotypic interactions of spinster with the genes encoding proteins for cell death control in Drosophila melanogaster. *Arch. Insect Biochem. Physiol.* **73**, 119-127.
Schnorrer, F., Schönbauer, C., Langer, C. C. H., Dietzl, G., Novatchkova, M., Schernhuber, K., Fellner, M., Azaryan, A., Radolf, M., Stark, A. et al. (2010). Systematic genetic analysis of muscle morphogenesis and function in Drosophila. *Nature* **464**, 287-291.
Schwab, S. R., Pereira, J. P., Matloubian, M., Xu, Y., Huang, Y. and Cyster, J. G. (2005). Lymphocyte sequestration through S1P lyase inhibition and disruption of S1P gradients. *Science* **309**, 1735-1739.
Shcherbata, H. R., Yatsenko, A. S., Patterson, L., Sood, V. D., Nudel, U., Yaffe, D., Baker, D. and Ruohola-Baker, H. (2007). Dissecting muscle and neuronal disorders in a Drosophila model of muscular dystrophy. *EMBO J.* **26**, 481-493.
Starz-Gaiano, M., Cho, N. K., Forbes, A. and Lehmann, R. (2001). Spatially restricted activity of a Drosophila lipid phosphatase guides migrating germ cells. *Development* **128**, 983-991.
Strub, G. M., Maceyka, M., Hait, N. C., Milstien, S. and Spiegel, S. (2010). Extracellular and intracellular actions of sphingosine-1-phosphate. *Adv. Exp. Med. Biol.* **688**, 141-155.
Taghli-Lamallem, O., Akasaka, T., Hogg, G., Nudel, U., Yaffe, D., Chamberlain, J. S., Ocorr, K. and Bodmer, R. (2008). Dystrophin deficiency in Drosophila reduces lifespan and causes a dilated cardiomyopathy phenotype. *Aging Cell* **7**, 237-249.
Udd, B., Vihola, A., Sarparanta, J., Richard, I. and Hackman, P. (2005). Titinopathies and extension of the M-line mutation phenotype beyond distal myopathy and LGMD2J. *Neurology* **64**, 636-642.
Yonamine, I., Bamba, T., Nirala, N. K., Jesmin, N., Kosakowska-Cholody, T., Nagashima, K., Fukusaki, E., Acharya, J. K. and Acharya, U. (2011). Sphingosine kinases and their metabolites modulate endolysosomal trafficking in photoreceptors. *J. Cell Biol.* **192**, 557-567.
Zhang, N., Zhang, J., Cheng, Y. and Howard, K. (1996). Identification and genetic analysis of wunen, a gene guiding Drosophila melanogaster germ cell migration. *Genetics* **143**, 1231-1241.
Zhang, N., Zhang, J., Purcell, K. J., Cheng, Y. and Howard, K. (1997). The Drosophila protein Wunen repels migrating germ cells. *Nature* **385**, 64-67.